J|A|C|S ARTICLES

Published on Web 03/12/2010

# Switchable Nile Red-Based Probe for Cholesterol and Lipid Order at the Outer Leaflet of Biomembranes

Oleksandr A. Kucherak, Sule Oncul,[†] Zeinab Darwich, Dmytro A. Yushchenko, Youri Arntz, Pascal Didier, Yves Mély, and Andrey S. Klymchenko*

*Laboratoire de Biophotonique et Pharmacologie, UMR 7213 CNRS, Université de Strasbourg, Faculté de Pharmacie, 74, Route du Rhin, 67401 Illkirch Cedex, France*

Received January 14, 2010; E-mail: andrey.klymchenko@unistra.fr

***Abstract:*** Cholesterol and sphingomyelin form together a highly ordered membrane phase, which is believed to play important biological functions in plasma membranes of mammalian cells. Since sphingomyelin is present mainly at the outer leaflet of cell membranes, monitoring its lipid order requires molecular probes capable to bind specifically at this leaflet and exhibit negligibly slow flip-flop. In the present work, such a probe was developed by modifying the solvatochromic fluorescent dye Nile Red with an amphiphilic anchor group. To evaluate the flip-flop of the obtained probe (NR12S), we developed a methodology of reversible redox switching of its fluorescence at one leaflet using sodium dithionite. This method shows that NR12S, in contrast to parent Nile Red, binds exclusively the outer membrane leaflet of model lipid vesicles and living cells with negligible flip-flop in the time scale of hours. Moreover, the emission maximum of NR12S in model vesicles exhibits a significant blue shift in liquid ordered phase (sphingomyelin-cholesterol) as compared to liquid disordered phase (unsaturated phospholipids). As a consequence, these two phases could be clearly distinguished in NR12S-stained giant vesicles by fluorescence microscopy imaging of intensity ratio between the blue and red parts of the probe emission spectrum. Being added to living cells, NR12S binds predominantly, if not exclusively, their plasma membranes and shows an emission spectrum intermediate between those in liquid ordered and disordered phases of model membranes. Importantly, the emission color of NR12S correlates well with the cholesterol content in cell membranes, which allows monitoring the cholesterol depletion process with methyl-$\beta$-cyclodextrin by fluorescence spectroscopy and microscopy. The attractive photophysical and switching properties of NR12S, together with its selective outer leaflet staining and sensitivity to cholesterol and lipid order, make it a new powerful tool for studying model and cell membranes.

## Introduction

The structure and function of cell plasma membranes is largely controlled by their lipid composition and particularly by cholesterol, which represents up to 40% of the lipids in plasma membranes.[1] Cholesterol interacts strongly with phospholipids in membranes and, notably, with sphingomyelin (SM), another major lipid component of cell membranes.[2−4] Cholesterol and SM form a highly packed state, called liquid ordered (Lo) phase, in lipid bilayers. This phase is clearly separated in model membranes from the loosely packed liquid disordered (Ld) phase formed by unsaturated lipids and cholesterol.[5] The presence of Lo domains (or rafts) in cell plasma membranes was hypothesized from the discovery of detergent-insoluble membrane fractions enriched with SM, saturated phospholipids, and cholesterol.[6] This hypothesis stimulated intensive research and debates,[1−7] since their evidence was mainly provided from indirect techniques,[8] while their direct visualization remains a challenge. Estimation of the fraction of Lo phase in cell

[†] Present address: Acibadem University, School of Medicine, Department of Biophysics, Fevzi Cakmak Cd. Divan Sk. No. 1, 34848 Maltepe, Istanbul, Turkey.

(1) (a) Yeagle, P. L. *Biochim. Biophys. Acta* **1985**, *822*, 267–287. (b) Simons, K.; Ikonen, E. *Nature* **1997**, *387*, 569–572. (c) Simons, K.; Ikonen, E. *Science* **2000**, *290*, 1721–1726. (d) Brown, D. A.; London, E. *J. Membr. Biol.* **1998**, *164*, 103–114. (e) Brown, D. A.; London, E. *J. Biol. Chem.* **2000**, *275*, 17221–17224. (f) Ohvo-Rekila, H.; Ramstedt, B.; Leppimaki, P.; Peter Slotte, J. *Prog. Lipid Res.* **2002**, *41*, 66–97. (g) Maxfield, F. R.; Tabas, I. *Nature* **2005**, *438*, 612–621.

(2) (a) Lange, Y.; Ye, J.; Rigney, M.; Steck, T. *J. Biol. Chem.* **2000**, *275*, 17468–17475. (b) Lange, Y.; Swaisgood, M. H.; Ramos, B. V.; Steck, T. L. *J. Biol. Chem.* **1989**, *264*, 3786–3793.

(3) (a) Radhakrishnan, A.; McConnell, H. M. *J. Am. Chem. Soc.* **1999**, *121*, 486–487. (b) McConnell, H. M.; Radhakrishnan, A. *Biochim. Biophys. Acta* **2003**, *1610*, 159–173.

(4) Sankaram, M. B.; Thompson, T. E. *Biochemistry* **1990**, *29*, 10670–10675.

(5) (a) Dietrich, C.; Bagatolli, L. A.; Volovyk, Z. N.; Thompson, N. L.; Levi, M.; Jacobson, K.; Gratton, E. *Biophys. J.* **2001**, *80*, 1417–1428. (b) Veatch, S. L.; Keller, S. L. *Phys. Rev. Lett.* **2002**, *89*, 268101. (c) Veatch, S. L.; Keller, S. L. *Biophys. J.* **2003**, *85*, 3074–3083. (d) Baumgart, T.; Hess, S. T.; Webb, W. W. *Nature* **2003**, *425*, 821–824. (e) Ahmed, S. N.; Brown, D. A.; London, E. *Biochemistry* **1997**, *36*, 10944–10953. (f) De Almeida, R. F. M.; Fedorov, A.; Prieto, M. *Biophys. J.* **2003**, *85*, 2406–2416.

(6) (a) Brown, D. A.; Rose, J. K. *Cell* **1992**, *68*, 533–544. (b) Schroeder, R.; London, E.; Brown, D. *Proc. Natl. Acad. Sci. U.S.A.* **1994**, *91*, 12130–12134. (c) London, E.; Brown, D. A. *Biochim. Biophys. Acta* **2000**, *1508*, 182–195.

(7) (a) Simons, K.; Toomre, D. *Nat. Rev. Mol. Cell Biol.* **2000**, *1*, 31–39. (b) Brown, D. A.; London, E. *Annu. Rev. Cell Dev. Biol.* **1998**, *14*, 111–136. (c) Field, K. A.; Holowka, D.; Baird, B. *J. Biol. Chem.* **1997**, *272*, 4276–4280. (d) Hanzal-Bayer, M. F.; Hancock, J. F. *FEBS Lett.* **2007**, *581*, 2098–2104. (e) Tian, T.; Harding, A.; Inder, K.; Plowman, S.; Parton, R. G.; Hancock, J. F. *Nat. Cell Biol.* **2007**, *9*, 875–877.

  

membranes ranges from 10% to 80%, depending on the method used for its quantification. The difficulties to characterize Lo phase in cell membranes are first connected with their complex lipid composition, the presence of membrane proteins and cytoskeleton.[9] The second complication raises from the asymmetric distribution of lipids between the two leaflets. Indeed, while the outer leaflet contains a large amount of SM (up to 40%), its fraction in the inner leaflet is marginal.[10] Therefore, correct evaluation of Lo phase requires high specificity to this phase as well as high selectivity to the outer membrane leaflet.

To characterize the cholesterol content in membranes, the most classical method is to directly measure the lipid composition by isolation of cell plasma membrane fractions.[2] However, it is an invasive method, which does not allow real-time in situ measurements and may lead to artifacts because cholesterol can migrate between different cellular compartments[1] during the membrane isolation. More recent approaches are based on the extraction of radiolabeled cholesterol by cyclodextrin[11] and cholesterol-oxidation by microelectrode,[12] which allow real-time kinetics measurements of cholesterol in cells. However, these methods cannot address the spatial distribution of Lo and Ld phases in lipid membranes.

Fluorescent probes are probably the most attractive tool to study Lo/Ld phase separation and lipid compositions in model and cell membranes. Two classes of probes are mainly used. The first class corresponds to probes that stain selectively the Lo phase in model vesicles. This class includes the fluorescently labeled cholera toxin B-subunit (CT-B),[8a,13] saturated phospholipids labeled with NBD[5a] or Cy5[14] and GFP-labeled glycosylphosphatidylinositol (GPI),[15] as well as fluorescent dyes with long alkyl chains, such as LcTMA-DPH,[16] diI-C20, or polycyclic probes such as Terrylene or Naphtopyrene.[17] Though these probes are useful for imaging the phase separation in model and cell membranes, they cannot provide information about the actual composition of the separated phases. The second class corresponds to environment-sensitive probes, such as Laurdan[18] and its derivatives,[19] di-4-ANEPPDHQ[20] and 3-hydroxyflavone derivatives.[21] These probes distribute in both Ld and Lo phases, and their emission color or intensity depends strongly on the local polarity/hydration or fluidity, which in turn is related to the lipid composition and the actual phase state of the membrane.[18] Thus, these probes provide a unique possibility to study the membrane phases in connection to their lipid composition. However, only a small number of these probes is really applicable to membranes of living cells,[19,20,22] because most of them internalize rapidly inside the cell. Moreover, the flip-flop of these probes is not clearly addressed in literature, since the flip-flop studies are mainly based on indirect measurements,[20,22] so that it is difficult to evaluate precisely the distribution of the probes between the two leaflets. Therefore, it still remains a challenge to develop an environment-sensitive fluorescent probe that stains exclusively the outer leaflet of cell membranes. In the present work, we selected Nile Red[23] (Chart 1) as an environment-sensitive fluorophore for designing this fluorescent probe. Nile Red shows a number of attractive features, such as high fluorescence quantum yield, suitable excitation wavelength for application with common lasers and satisfactory photostability.[24] This dye found a variety of applications to characterize hydrophobic domains of proteins, dendrimers, micelles and model lipid membranes.[25] However, it cannot be used for studying cell plasma membranes, because it internalizes readily inside the cell and binds specifically to lipid droplets,[23] which are the most apolar cell compartments. Recently, we showed that a selective localization of a hydrophobic fluorophore at the plasma membrane can be achieved


(8) (a) Dietrich, C.; Yang, B.; Fujiwara, T.; Kusumi, A.; Jacobson, K. *Biophys. J.* **2002**, *82*, 274–284. (b) Pralle, A.; Keller, P.; Florin, E. L.; Simons, K.; Horber, J. K. *J. Cell. Biol.* **2000**, *148*, 997–1008. (c) Schultz, G. J.; Kada, G.; Pastushenko, V. P.; Schindler, H. *EMBO J.* **2000**, *19*, 892–901. (d) Lenne, P. F.; Wawrezinieck, L.; Conchonaud, F.; Wurtz, O.; Boned, A.; Guo, X. J.; Rigneault, H.; He, H. T.; Marguet, D. *EMBO J.* **2006**, *25*, 3245–3256. (e) Wawrezinieck, L.; Rigneault, H.; Marguet, D.; Lenne, P. F. *Biophys. J.* **2005**, *89*, 4029–4042. (f) Swamy, M. J.; Ciani, L.; Ge, M.; Smith, A. K.; Holowka, D.; Baird, B.; Freed, J. H. *Biophys. J.* **2006**, *90*, 4452–4465.

(9) Kusumi, A.; Sako, Y. *Curr. Opin. Cell Biol.* **1996**, *8*, 566–574.

(10) (a) Van Meer, G. *Annu. Rev. Cell Biol.* **1989**, *5*, 247–275. (b) Zwaal, R. F.; Schroit, A. J. *Blood* **1997**, *89*, 1121–1132.

(11) (a) Haynes, M. P.; Phillips, M. C.; Rothblat, G. H. *Biochemistry* **2000**, *39*, 4508–4517. (b) Lange, Y.; Ye, J.; Steck, T. L. *Proc. Natl. Acad. Sci. U.S.A.* **2004**, *101*, 11664–11667.

(12) Jiang, D.; Devadoss, A.; Palencsár, M. S.; Fang, D.; White, N. M.; Kelley, T. J.; Smith, J. D.; Burgess, J. D. *J. Am. Chem. Soc.* **2007**, *129*, 11352–11353.

(13) (a) Janes, P. W.; Ley, S. C.; Magee, A. I. *J. Cell. Biol.* **1999**, *147*, 447–461. (b) Kenworthy, A. K.; Petranova, N.; Edidin, M. *Mol. Biol. Cell* **2000**, *11*, 1645–1655.

(14) Schultz, G. J.; Kada, G.; Pastushenko, V. P.; Schindler, H. *EMBO J.* **2000**, *19*, 892–901.

(15) (a) Sharma, P.; Varma, R.; Sarasij, R. C.; Ira; Gousset, K.; Krishnamoorthy, G.; Rao, M.; Mayor, S. *Cell* **2004**, *116*, 577–589. (b) Vrljic, M.; Nishimura, S. Y.; Brasselet, S.; Moerner, W. E.; McConnell, H. M. *Biophys. J.* **2002**, *83*, 2681–2692. (c) Kenworthy, A. K.; Nichols, B. J.; Remmert, C. L.; Hendrix, G. M.; Kumar, M.; Zimmerberg, J.; Lippincott-Schwartz, J. *J. Cell. Biol.* **2004**, *165*, 735–46.

(16) (a) Haluska, C. K.; Schröder, A. P.; Didier, P.; Heissler, D.; Duportail, G.; Mély, Y.; Marques, C. M. *Biophys. J.* **2008**, *95*, 5737–5747. (b) Xu, X.; Bittman, R.; Duportail, G.; Heissler, D.; Vilchéze, C.; London, E. *J. Biol. Chem.* **2001**, *276*, 33540–33546.

(17) (a) Korlach, J.; Schwille, P.; Webb, W. W.; Feigenson, G. W. *Proc. Natl. Acad. Sci. U.S.A.* **1999**, *96*, 8461–8466. (b) Baumgart, T.; Hunt, G.; Farkas, E. R.; Webb, W. W.; Feigenson, G. W. *Biochim. Biophys. Acta* **2007**, *1768*, 2182–2194.

(18) (a) Bagatolli, L. A. *Biochim. Biophys. Acta* **2006**, *1758*, 1541–1556. (b) Parasassi, T.; Gratton, E.; Yu, W. M.; Wilson, P.; Levi, M. *Biophys. J.* **1997**, *72*, 2413–2429. (c) Gaus, K.; Gratton, E.; Kable, E. P. W.; Jones, A. S.; Gelissen, I.; Kritharides, L.; Jessup, W. *Proc. Natl. Acad. Sci. U.S.A.* **2003**, *100*, 15554–15559.

(19) (a) Kim, H. M.; Choo, H.-J.; Jung, S.-Y.; Ko, Y.-G.; Park, W.-H.; Jeon, S.-J.; Kim, C. H.; Joo, T.; Cho, B. R. *ChemBioChem* **2007**, *8*, 553–559. (b) Kim, H. M.; Jeong, B. H.; Hyon, J.-Y.; An, M. J.; Seo, M. S.; Hong, J. H.; Lee, K. J.; Kim, C. H.; Joo, T.; Hong, S.-C.; Cho, B. R. *J. Am. Chem. Soc.* **2008**, *130*, 4246–4247.

(20) (a) Jin, L.; Millard, A. C.; Wuskell, J. P.; Clark, H. A.; Loew, L. M. *Biophys. J.* **2005**, *89*, L4–L6. (b) Jin, L.; Millard, A. C.; Wuskell, J. P.; Dong, X.; Wu, D.; Clark, H. A.; Loew, L. M. *Biophys. J.* **2006**, *90*, 2563–2575.

(21) (a) Klymchenko, A. S.; Oncul, S.; Didier, P.; Schaub, E.; Bagatolli, L.; Duportail, G.; Mély, Y. *Biochim. Biophys. Acta* **2009**, *1788*, 495–499. (b) M'Baye, G.; Mély, Y.; Duportail, G.; Klymchenko, A. S. *Biophys. J.* **2008**, *95*, 1217–25. (c) Klymchenko, A. S.; Mély, Y.; Demchenko, A. P.; Duportail, G. *Biochim. Biophys. Acta* **2004**, *1665*, 6–19.

(22) Shynkar, V. V.; Klymchenko, A. S.; Kunzelmann, C.; Duportail, G.; Muller, C. D.; Demchenko, A. P.; Freyssinet, J.-M.; Mély, Y. *J. Am. Chem. Soc.* **2007**, *129*, 2187–2193.

(23) (a) Greenspan, P.; Mayer, E. P.; Fowler, S. D. *J. Cell. Biol.* **1985**, *100*, 965–973. (b) Diaz, G.; Melis, M.; Batetta, B.; Angius, F.; Falchi, A. *Micron* **2008**, *39*, 819–824.

(24) Greenspan, P.; Fowler, S. D. *J. Lipid Res.* **1985**, *26*, 781–789.

(25) (a) Lampe, J. N.; Fernandez, C.; Nath, A.; Atkins, W. M. *Biochemistry* **2008**, *47*, 509–516. (b) Gillies, E. R.; Jonsson, T. B.; Freíchet, Jean M. J. *J. Am. Chem. Soc.* **2004**, *126*, 11936–11943. (c) Maiti, N. C.; Krishna, M. M. G.; Britto, P. J.; Periasamy, N. *J. Phys. Chem. B* **1997**, *101*, 11051–11060. (d) Freeman, D. M.; Kroe, R. R.; Ruffles, R.; Robson, J.; Coleman, J. R.; Grygon, C. A. *Biophys. J.* **2001**, *80*, 2375. (e) Gao, F.; Mei, E.; Lim, M.; Hochstrasser, R. M. *J. Am. Chem. Soc.* **2006**, *128*, 4814–4822. (f) Nath, A.; Koo, P. K.; Rhoades, E.; Atkins, W. M. *J. Am. Chem. Soc.* **2008**, *130*, 15746–15747. (g) Chen, G.; Guan, Z. *J. Am. Chem. Soc.* **2004**, *126*, 2662–2663. (h) Mukherjee, S.; Raghuraman, H.; Chattopadhyay, A. *Biochim. Biophys. Acta* **2007**, *1768*, 59–66.

***Chart 1.*** Probes Nile Red and NR12S and Their Hypothetic Localization with Respect to Lipids (Blue) in Membranes; Anchor Part of the NR12S Probe Is in Red

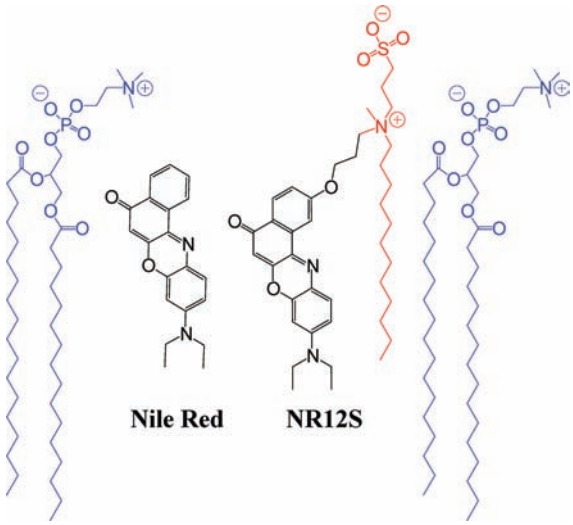


by conjugating it with a zwitterionic group and a long hydrophobic chain.[22] Though the obtained probe was hypothesized to bind to the outer biomembrane leaflet without further fast flip-flop, we could not provide a direct evidence for this.

In the present work, using the same design, we developed a new Nile Red based probe for cell plasma membranes. Moreover, using a unique switching property of Nile Red fluorophore that was not reported before, we showed that, unlike the parent Nile Red, the novel probe stains exclusively the outer leaflet of lipid vesicles and cells. Furthermore, the probe was found to exhibit strongly different emission in Lo and Ld phases, and in living cells, its emission color varies with the cholesterol content. Thus, this probe constitutes a new tool for quantification of cholesterol-rich Lo phase in cell plasma membranes.

## Materials and Methods

All chemicals and solvents for synthesis were from Sigma-Aldrich. Synthesis of NR12S is described in Supporting Information.

**Lipid Vesicles.** Dioleoylphosphatidylcholine (DOPC), dioleoylphosphatidylserine (DOPS), and cholesterol were purchased from Sigma-Aldrich. Bovine brain sphingomyelin (SM) was from Avanti Polar Lipids (Alabaster, AL). Large unilamellar vesicles (LUVs) were obtained by the extrusion method as previously described.[26] Briefly, a suspension of multilamellar vesicles was extruded by using a Lipex Biomembranes extruder (Vancouver, Canada). The size of the filters was first 0.2 $\mu$m (7 passages) and thereafter 0.1 $\mu$m (10 passages). This generates monodisperse LUVs with a mean diameter of 0.11 $\mu$m as measured with a Malvern Zetamaster 300 (Malvern, U.K.). LUVs were labeled by adding aliquots (generally 2 $\mu$L) of probe stock solutions in dimethyl sulfoxide to 1-mL solutions of vesicles. Since the probe binding kinetics is very rapid, the fluorescence experiments were performed a few minutes after addition of the aliquot. A 20 mM phosphate buffer, pH 7.4, was used in these experiments. Concentrations of the probes and lipids were generally 1 and 200 $\mu$M, respectively.

Giant unilamellar vesicles (GUVs) were generated by electroformation in a home-built liquid cell (University of Odense, Denmark), using previously described procedures.[27] A 0.1 mM solution of lipids in chloroform was deposited on the platinum wires of the chamber, and the solvent was evaporated under vacuum for 30 min. The chamber, thermostatted at 55 °C, was filled with a 300 mM sucrose solution, and a 2-V, 10-Hz alternating electric current was applied to this capacitor-like configuration for ca. 2 h. Then, a 50 $\mu$L aliquot of the obtained stock solution of GUVs in sucrose (cooled down to room temperature) was added to 200 $\mu$L of 300 mM glucose solution to give the final suspension of GUVs used in microscopy experiments. The staining of GUVs was performed by addition of an aliquot of the probe stock solution in DMSO to obtain a 0.1 $\mu$M final probe concentration (final DMSO volume <0.25%).

**Reversible Bleaching of Nile Red and NR12S with Sodium Dithionite and Flip-Flop Studies.** A 1 M stock solution of sodium dithionite in 1 M Tris was used for the experiments. To 1 mL of 5 $\mu$M solution of Nile Red or NR12S in a 1:1 (v/v) ethanol/water mixture in a quartz cuvette was added an aliquot of the stock solution of dithionite to a final concentration 2 mM. Then, approximately 25 mL of air was applied to this solution through a syringe for approximately 20 s. The procedure of dithionite and air treatment was repeated several times. During all steps of this cyclic treatment, the absorbance at 590 nm (Nile Red) was measured as a function of time. For the flip-flop studies, DOPC LUVs were labeled with probes Nile Red and NR12S by two different methods. In method 1, the probe was mixed with lipids in chloroform, and the vesicles were prepared from this mixture as described above. This method ensured symmetric distribution of the probe between both leaflets. In method 2, the probe was added to 0.5 mL of buffer and then mixed with 0.5 mL of suspension of nonlabeled vesicles and incubated at room temperature for 5 min, which allowed initial staining of the outer membrane leaflet. The final probe concentration for both methods was 1 $\mu$M. To study the flip-flop kinetics, the fraction (%) of NR12S probe flipped from the outer to the inner leaflet in LUVs was evaluated as a function of time at 20 and 37 °C. The suspension of LUVs was stained with a probe by method 2. After a given incubation time (at 20 or 37 °C), the fluorescence intensities at 610 nm before ($I_0$) and 3 min after addition of 10 mM sodium dithionite ($I_{DT}$) were measured. The fraction of flipped probe for a given incubation time was expressed as $I_{DT}/I_0 \times 100\%$.

**Cell Lines, Culture Conditions, and Treatment.** The U87MG human glioblastoma cell line (ATCC) was cultured in Eagle's minimal essential medium (EMEM from LONZA) with 10% heat-inactivated fetal bovine serum (PAN Biotech GmbH) and 0.6 mg/mL glutamine (Biowhittaker) at 37 °C in a humidified 5% $CO_2$ atmosphere. Cell concentration of $5-10 \times 10^4$ cells/mL was maintained by removal of a portion of the culture and replacement with fresh medium 3 times per week. Cholesterol depletion and enrichment of cell membranes was performed using methyl-$\beta$-cyclodextrin (M$\beta$CD) and M$\beta$CD−cholesterol complex (Sigma-Aldrich), respectively, according to described procedures.[28] Briefly, stock solutions of M$\beta$CD and M$\beta$CD−cholesterol complex in Dulbecco's phosphate-buffered saline (DPBS) were prepared at a suitable concentration, filtered by Millipore filter (0.2 $\mu$m), and added to the cells to a final concentration of 5 mM. The treated cells were kept in the incubator at 37 °C for 30 min or 2 h.

In fluorescence spectroscopy experiments, cells were detached by trypsinization. EMEM medium was first removed from the culture dish, and cells were washed two times with DPBS. Trypsin 10x (LONZA) solution was diluted 10 times by DPBS and incubated with the cells at 37 °C for 4 min. The solution of trypsinized cells was then diluted by DPBS, transferred to Falcon tubes and centrifuged at 1500 rpm for 5 min. The washing procedure was repeated one more time with HBSS solution. To stain the cell suspension with the NR12S probe, an appropriate aliquot of its stock

(26) Hope, M. J.; Bally, M. B.; Webb, G.; Cullis, P. R. *Biochim. Biophys. Acta* **1985**, *812*, 55–65.

(27) (a) Angelova, M. I.; Dimitrov, D. S. *Faraday Discuss.* **1986**, *81*, 303–311. (b) Fidorra, M.; Duelund, L.; Leidy, C.; Simonsen, A. C.; Bagatolli, L. A. *Biophys. J.* **2006**, *90*, 4437–4451. (c) Kahya, N.; Scherfeld, D.; Bacia, K.; Poolman, B.; Schwille, P. *J. Biol. Chem.* **2003**, *278*, 28109–28115.

(28) Zidovetzki, R.; Levitan, I. *Biochim. Biophys. Acta* **2007**, *1768*, 1311–1324.

solution in DMSO was added to 0.5 mL of HBSS buffer, and after vortexing the solution was immediately added to 0.5 mL of the cell suspension to obtain a final probe concentration of 0.1 $\mu$M (<0.25% DMSO) and a cell concentration of $5 \times 10^5-10^6$ cells/mL. It should be noted that only freshly prepared solutions of the probe in HBSS should be used (<1 min) for cell staining, because of the slow aggregation of the probe in water. Before measurements, the cell suspension with probe was incubated for 7 min at room temperature in the dark. For the microscopy studies, attached cells were washed two times by gentle rinsing with HBSS. A freshly prepared solution of NR12S or Nile Red in HBSS was then added to the cells to a final concentration of 0.3 $\mu$M (<0.25% DMSO volume) and incubated for 7 min in the dark at room temperature.

**Fluorescence Spectroscopy and Microscopy.** Absorption spectra were recorded on a Cary 4 spectrophotometer (Varian) and fluorescence spectra on a FluoroMax 3.0 (Jobin Yvon, Horiba) spectrofluorometer. Fluorescence emission spectra were systematically recorded at 520 nm excitation wavelength at room temperature, unless indicated. All the spectra were corrected from the fluorescence of the corresponding blank (suspension of cells or lipid vesicles without the probe). Fluorescence quantum yields (QY) were measured using solution of Nile Red in methanol as a reference (QY = 38%).[29] Fluorescence microscopy experiments were performed by using a home-built two-photon laser scanning setup based on an Olympus IX70 inverted microscope with an Olympus 60x 1.2NA water immersion objective.[30] Two-photon excitation was provided by a titanium-sapphire laser (Tsunami, Spectra Physics), and photons were detected with Avalanche Photodiodes (APD SPCM-AQR-14-FC, Perkin-Elmer) connected to a counter/timer PCI board (PCI6602, National Instrument). Imaging was carried out using two fast galvo mirrors in the descanned fluorescence collection mode. Typical acquisition time was 5 s with an excitation power around 2.5 mW ($\lambda$ = 830 nm) at the sample level. Images corresponding to the blue and red channels were recorded simultaneously using a dichroic mirror (Beamsplitter 585 DCXR) and two APDs. The images were processed with a homemade program under LabView that generates a ratiometric image by dividing the image of the blue channel by that of the red channel. For each pixel, a pseudocolor scale is used for coding the ratio, while the intensity is defined by the integral intensity recorded for both channels at the corresponding pixel.[21a]

## Results and Discussion

**Design and Synthesis.** The design of the new probe NR12S (Chart 1) is based on the conjugation of the Nile Red fluorophore with an anchor group, which was recently proposed for localizing 3-hydroxychromone dyes at the outer leaflet of the cell plasma membrane.[22] This anchor group is composed of a long alkyl chain and a zwitterionic group, allowing strong interactions with the lipid membranes and thus their specific staining.

To functionalize Nile Red, we prepared 2-hydroxy-substituted Nile Red from 5-(diethylamino)-2-nitrosophenol and naphthalene-1,6-diol according to an available procedure.[31] The obtained 2-hydroxy-Nile Red was alkylated with 1-bromo-3-chloropropane. The product was further reacted with dodecylmethylamine, and the obtained tertiary amine was then quaternized by 1,3-propane sultone affording the final probe NR12S (see Supporting Information).

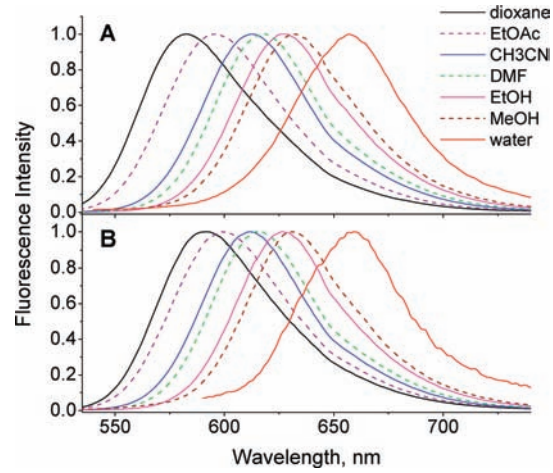


***Figure 1.*** Normalized fluorescence spectra of Nile Red (A) and NR12S (B) in different solvents.

***Table 1.*** Spectroscopic Properties of Studied Dyes in Organic Solvents[a]

| | | dye | | | | | |
|---|---|---|---|---|---|---|---|
| | | Nile Red | | | NR12S | | |
| solvent | $E_T(30)$ | $\lambda_{abs}$, nm | $\lambda_{fluor}$, nm | QY, % | $\lambda_{abs}$, nm | $\lambda_{fluo}$, nm | QY, % |
| dioxane | 36.0 | 520 | 583 | 91 | 526 | 592 | 74 |
| EtOAc | 38.1 | 525 | 595 | 87 | 527 | 599 | 84 |
| THF | 37.4 | 530 | 595 | 90 | 530 | 597 | 81 |
| $CH_2Cl_2$ | 40.7 | 541 | 601 | 88 | 542 | 602 | 80 |
| DMF | 43.2 | 544 | 618 | 63 | 544 | 615 | 69 |
| DMSO | 45.1 | 554 | 629 | 46 | 554 | 627 | 55 |
| $CH_3CN$ | 45.6 | 536 | 612 | 82 | 536 | 612 | 81 |
| EtOH | 51.9 | 550 | 626 | 52 | 550 | 626 | 52 |
| MeOH | 55.4 | 553 | 632 | 38[b] | 555 | 631 | 40 |
| buffer | 63.1 | 591 | 657 | 5.0 | 521 | 657 | 0.2 |

[a] $\lambda_{abs}$ and $\lambda_{fluor}$, are absorption and emission maxima, respectively. Buffer refers to a 20 mM phosphate buffer (pH 7.4). [b] The QY value is from ref 29.

**Characterization in Solvents.** The spectroscopic properties of NR12S were studied in comparison to the parent Nile Red in different organic solvents. The absorption and fluorescence spectra of the two dyes were highly similar (Figure 1), especially in solvents of medium polarity. Moreover, both dyes show a similar strong red shift of their emission on increase in solvent polarity. However, differences in the emission spectra were observed in less polar solvents (dioxane and ethyl acetate), which could be connected with the effect of the proximal polar charged group.[32]

Similarly to the parent Nile Red, NR12S shows high fluorescence QY in most organic solvents (Table 1). Remarkably, in aqueous buffer NR12S is almost nonfluorescent (QY = 0.2%), whereas Nile Red is significantly fluorescent (QY = 5.0%). This could be explained by the detergent-like structure of NR12S, so that in water it may form oligomers or micelles, where its fluorophore is probably self-quenched. The existence of NR12S oligomers in water is also supported by the strongly blue-shifted absorption maximum in water as compared to that in organic solvents (Table 1). A similar quenching in water was observed for 3-hydroxyflavone derivatives bearing an amphiphilic group analogous to NR12S.[22,32b]

(29) Deda, M. L.; Ghedini, M.; Aiello, I.; Pugliese, T.; Barigelletti, F.; Accorsi, G. *J. Organomet. Chem.* **2005**, *690*, 857–861.
(30) (a) Clamme, J.-P.; Azoulay, J.; Mély, Y. *Biophys. J.* **2003**, *84*, 1960–1968. (b) Azoulay, J.; Clamme, J.-P.; Darlix, J.-L.; Roques, B. P.; Mely, Y. *J. Mol. Biol.* **2003**, *326*, 691–700.
(31) (a) Martin-Brown, S. A.; Fu, Y.; Saroja, G.; Collinson, M. M.; Higgins, D. A. *Anal. Chem.* **2005**, *77*, 486–494. (b) Briggs, M. S. J.; Bruce, I.; Miller, J. N.; Moody, C. J.; Simmonds, A. C.; Swann, E. *J. Chem. Soc. Perkin Trans. 1* **1997**, 1051–1058.
(32) (a) Klymchenko, A. S.; Demchenko, A. P. *J. Am. Chem. Soc.* **2002**, *124*, 12372–12379. (b) Klymchenko, A. S.; Duportail, G.; Ozturk, T.; Pivovarenko, V. G.; Mély, Y.; Demchenko, A. P. *Chem. Biol.* **2002**, *9*, 1199–1208.

***Table 2.*** Spectroscopic Properties of Nile Red and NR12S in Lipid Vesicles[a]

| | | dye | | | | | |
|---|---|---|---|---|---|---|---|
| | | Nile Red | | | NR12S | | |
| composition | phase state | $\lambda_{abs}$, nm | $\lambda_{fluo}$, nm | QY, % | $\lambda_{abs}$, nm | $\lambda_{fluo}$, nm | QY, % |
| DOPC | Ld | 549 | 628 | 42 | 530 | 608 | 48 |
| DOPC/CL | Ld | 550 | 624 | 48 | 527 | 605 | 47 |
| DPPC | L$\beta$ | 550 | 608 | 34 | 527 | 599 | 8 |
| DPPC/CL | Lo | 552 | 595 | 60 | 521 | 556 | 32 |
| DPPC/CL (60) | Ld | | 603 | 72 | | 601 | 57 |
| SM | L$\beta$ | 543 | 617 | 40 | 528 | 596 | 18 |
| SM/CL | Lo | 530 | 586 | 45 | 521 | 572 | 30 |
| SM/CL (60) | Ld | | 612 | 53 | | 593 | 45 |
| DOPS | Ld | 553 | 628 | 41 | 532 | 606 | 50 |

[a] $\lambda_{abs}$ and $\lambda_{fluor}$ are absorption and emission maxima, respectively. All spectra were recorded at 20 °C, except those marked "(60)", which were recorded at 60 °C. In lipid mixtures, the cholesterol/lipid ratio was 1:2, mol/mol. Ld, Lo, and L$\beta$ correspond to liquid disordered, liquid ordered, and solid gel phases.

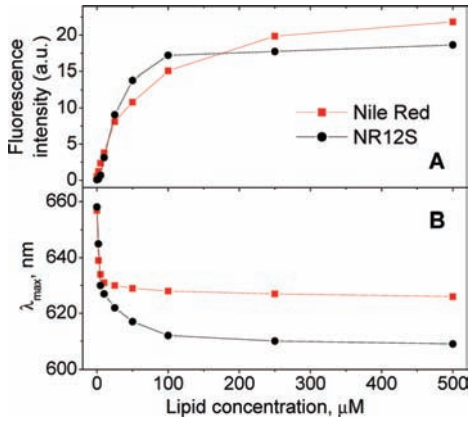


***Figure 2.*** Fluorescence of Nile Red and NR12S probes at different concentrations of DOPC LUVs. Integral intensity (A) and position of the maximum (B) vs DOPC concentration (phosphate buffer 20 mM, pH 7.4). Probe concentration was 0.5 $\mu$M.

**Binding to Lipid Vesicles.** Binding of the NR12S probe to DOPC lipid vesicles results in an about 200-fold increase of its fluorescence intensity, as can be seen from the quantum yields in aqueous buffer and in lipid vesicles (Tables 1 and 2). With the parent Nile Red, this increase is much less pronounced (only ca. 8-fold) due to its relatively high quantum yield in aqueous buffer. Therefore, NR12S dye is advantageous as a membrane probe, since unlike Nile Red its background fluorescence from the buffer can be neglected. The high fluorescence quantum yield of NR12S in lipid vesicles indicates that the probe oligomerization in water is likely reversible, so that an efficient membrane staining is achieved without additional solubilization techniques (with detergents or cyclodextrins). Moreover, titrations (Figure 2A) show that on increase in the lipid concentration, the fluorescence intensity of NR12S grows steeply and saturates at a probe/lipid ratio of 1:200, while for Nile Red this increase is less steep and saturation is reached only at a probe/lipid ratio 1:1000. These results suggest that NR12S binds more strongly to lipid membranes than Nile Red as a result of its amphiphilic anchor group. In addition, the position of the emission maximum of NR12S in DOPC LUVs at low probe/lipid ratio ($\leq$1:200) is significantly blue-shifted (17 nm) with respect to Nile Red (Figure 2B), indicating a deeper embedding of the fluorophore in the bilayer. However, at high probe/lipid ratios ($\geq$1:10), the emission maximum of NR12S becomes nearly the same as that of Nile Red, suggesting that the excess of NR12S probe binds nonspecifically to DOPC lipid bilayers and exhibits a shallower fluorophore insertion, similar to that of Nile Red.

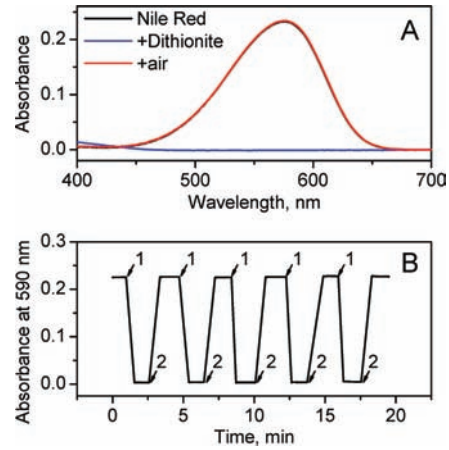


***Figure 3.*** On/off redox switching of Nile Red by dithionite/air treatment. (A) Absorption spectra of Nile Red in ethanol/water mixture (1:1, v/v) before treatment, after addition of 2 mM dithionite, and after further bubbling of air for 20 s. Extended spectral data are presented in Supporting Information. (B) Absorbance at 590 nm of Nile Red solution (ethanol/water) on repetitive treatment with 2 mM dithionite (1) and air bubbling (2). Inclined lines in (B) are used only for convenient presentation (connecting the experimental data points) and do not represent the transition kinetics between the low and high values of absorbance.

**Flip-Flop Studies Using Nile Red Reversible Bleaching with Dithionite.** One important issue in application of biomembrane probes is to evaluate their ability to stain selectively the outer membrane leaflet without fast flip-flop redistributing the dye between both leaflets. This problem was previously addressed for lipids modified with the NBD[33] fluorophore or spin-labels[34] using reducing agents, sodium dithionite and ascorbate, respectively, which inactivate the labels selectively in the outer leaflet of lipid vesicles. Though Nile Red is a chemically stable dye, it contains a quinoid fragment, which is a potential target for reduction. Moreover, the Nile Red analogues Nile Blue and resorufin can be reversibly reduced by different agents,[35] including dithionite. We checked the ability of Nile Red to be reduced by sodium dithionite in water/ethanol (1:1, v/v) solution. Addition of 2 mM dithionite leads to a complete disappearance of the absorption band of Nile Red (Figure 3A). Remarkably, after bubbling of air through this sample, the absorption band is fully recovered. This indicates that bleaching of Nile Red by dithionite is a fully reversible reduction process, so that this fluorophore can be switched off and on in a well-controlled manner. Furthermore, our data show that the reduction−oxidation cycle can be repeated many times without noticeable loss of the fluorophore (Figure 3B). The same results were obtained with the NR12S dye (see Supporting Information).

(33) McIntyret, J. C.; Sleight, R. G. *Biochemistry* **1991**, *30*, 11819–11827.
(34) (a) Seigneuret, M.; Devaux, P. F. *Proc. Natl. Acad. Sci. U.S.A.* **1984**, *81*, 3751–3755. (b) Kornberg, R. D.; McConnell, H. M. *Biochemistry* **1971**, *10*, 1111–1120.
(35) (a) Lemmon, T. L.; Westall, J. C.; Ingle, J. D., Jr. *Anal. Chem.* **1996**, *68*, 947–953. (b) Gorodetsky, A. A.; Ebrahim, A.; Barton, J. K. *J. Am. Chem. Soc.* **2008**, *130*, 2924–2925. (c) Cincotta, L.; Foley, J. W.; Cincotta, A. H. *Cancer Res.* **1993**, *53*, 2571–2580. (d) Erb, R. E.; Ehlers, M. H. *J. Dairy Sci.* **1950**, *33*, 853–864. (e) Zhou, M.; Diwu, Z.; Panchuk-Voloshina, N.; Haugland, R. P. *Anal. Biochem.* **1997**, *253*, 162–168. (f) Talbot, J. D.; Barrett, J. N.; Barrett, E. F.; David, G. *J. Neurochem.* **2008**, *105*, 807–819.

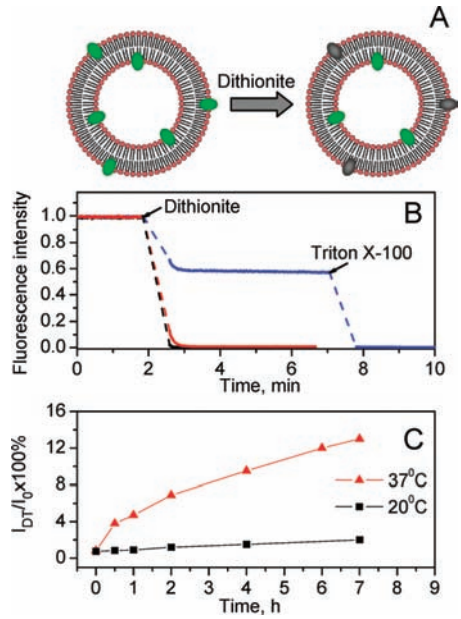


***Figure 4.*** Flip-flop studies of probes Nile Red and NR12S in DOPC LUVs using the dithionite bleaching method. (A) Schematic presentation of the selective bleaching of the probes at the outer leaflet of LUV by dithionite. (B) Evolution of the probe fluorescence intensity after addition of 10 mM dithionite and 1% (vol) of Triton X-100. Dyes were added to lipids either before LUV preparation to achieve staining of both leaflets (Nile Red = black line, NR12S = blue line) or after LUV preparation to stain the outer leaflet (NR12S = red line). (C) Fraction (%) of NR12S probe flipped from the outer to the inner leaflet in LUVs as a function of time at 20 and 37 °C. The suspension of LUVs was stained with the probe by method 2. After a given incubation time (at 20 or 37 °C), the fluorescence intensities at 600 nm before ($I_0$) and 3 min after addition of 10 mM sodium dithionite ($I_{DT}$) were measured. The fraction of flipped probe for a given incubation time was expressed as $I_{DT}/I_0 \times 100\%$. The probes concentration for both methods was 1 $\mu$M.

Since sodium dithionite is unable to penetrate the lipid bilayers, it can bleach the Nile Red fluorophore exclusively on the external leaflet (Figure 4A) and thus allows evaluation of the probe flip-flop, as it was done previously with NBD-labeled lipids.[33] For this purpose, we stained the lipid membranes in two different ways. In method 1, the probe was mixed with lipids first and then the vesicles were prepared, which ensured its symmetric distribution between both leaflets. In method 2, the probe was added to the vesicles from the external bulk solution to target the outer membrane leaflet. When the parent Nile Red probe was distributed in both leaflets (method 1), the addition of 10 mM dithionite resulted in complete bleaching (Figure 4B). An identical result was observed when the dye was added to vesicles from the bulk water (method 2, data not shown). Thus, Nile Red undergoes probably a very fast flip-flop, so that addition of dithionite can rapidly bleach the dye located initially on both leaflets. In contrast, when dithionite was added to vesicles stained with NR12S symmetrically on both leaflets (method 1), the fluorescence intensity drops rapidly until approximately 50% of the initial value (Figure 4B) and then remains relatively stable. Further addition of Triton X-100, which disrupts the lipid vesicles, leads to complete disappearance of fluorescence. This result is fully in line with that previously reported for NBD-lipids,[33] indicating that selective bleaching of NR12S fluorophore at the outer leaflet was achieved (Figure 4A), while the other 50% of the probe at the inner leaflet remained intact. The stabilization of the fluorescence intensity at ca. 50% of its initial value suggests that NR12S does not flip

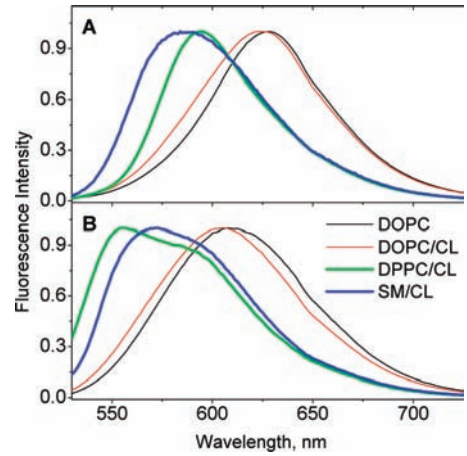


***Figure 5.*** Normalized fluorescence spectra of Nile Red (A) and NR12S (B) in LUVs of different lipid compositions. Probe and lipid concentrations were 1 and 200 $\mu$M, respectively.

to the outer leaflet within the experimental time. Importantly, when the staining was performed by addition of the probe to blank vesicles (method 2), the treatment with sodium dithionite resulted in rapid and complete bleaching (Figure 4B). The absence of residual fluorescence in this case clearly shows that NR12S stains exclusively the outer leaflet of vesicles and remains there at least within the incubation time (7 min, rt). We also incubated vesicles with the NR12S probe initially bound to the outer leaflet for longer time periods at 20 and 37 °C. Remarkably, at room temperature the residual fluorescence after dithionite treatment was still negligible even after 2 h of incubation and became significant (2%) only after 7 h of incubation (Figure 4C). Thus, at room temperature, the flip-flop process for NR12S is extremely slow. At 37 °C, the flip-flop was faster, though after 4 h only 9% of the probe migrated to the inner leaflet (Figure 4C).

Thus, according to our data, Nile Red redistributes between the two leaflets on the time scale of seconds or faster, whereas NR12S shows only marginal flip-flop for hours at room temperature. This dramatically decreased flip-flop dynamics of NR12S is evidently due to the anchor group containing a zwitterion and a long alkyl chain, which interact strongly with lipids, preventing the probe flip-flop. This is one of the first reports where a spontaneous binding of a nonlipidic membrane fluorescent probe to the outer leaflet is demonstrated by a chemical method. Previously, outer leaflet staining was suggested for styrylpyridinium and 3-hydroxyflavone dyes from their sensitivity to the transmembrane electric potential and lipid asymmetry, or detection of second harmonic generation signal in cell membranes.[20,22] It should be also noted that, similarly to our data in water/ethanol mixtures, the bleached NR12S probe in lipid vesicles can be further switched "on" by air bubbling. However, the fluorescence recovery in this case takes more time (data not shown).

**Sensitivity to Lipid Composition in Model Membranes.** Nile Red, being an environment-sensitive probe, shows a dependence of its spectrum on the lipid composition and the phase state in lipid bilayers (Figure 5). Since spectroscopic differences between the Lo and Ld phases are an important requirement for the development of probes for lipid domains,[18–21] the new probe NR12S was compared to Nile Red in these two phases. Similar to Nile Red, the new probe shows a significantly blue-shifted emission maximum in Lo phase vesicles composed of sphingomyelin and cholesterol (SM/CL) or DPPC and cholesterol

(DPPC/CL), compared to Ld phase vesicles composed of DOPC or DOPC/CL (Figure 5). These results are in line with other environment-sensitive probes such as Prodan, Laurdan,[18] di-4-ANEPPDHQ,[20] and 3-hydroxyflavone derivatives[21] showing a less polar and less hydrated environment in the Lo phase. Importantly, in DPPC and SM vesicles presenting gel phase ($L\beta$), the probes show intermediate positions of their emission maxima (Table 2). Thus, for both probes the emission maximum shifts to the blue in the following sequence of membrane phases: Ld → $L\beta$ → Lo, in line with recent data[20,21b] suggesting that the environment of these probes is the most dehydrated in the Lo phase.

An outstanding feature of the present dyes is that within the Ld phase, the position of their emission maximum is poorly sensitive to the presence of cholesterol (DOPC/CL vs DOPC, Figure 5, Table 2) Therefore, these dyes can clearly distinguish between cholesterol-rich Ld (DOPC/CL) and Lo (SM/CL or DPPC/CL) phases. In contrast, Prodan, Laurdan, 3-hydroxyflavone-based and di-4-ANEPPDHQ probes show a significant dependence of their spectra on the cholesterol content in the Ld phase,[18,20,36] so that the spectral differences between cholesterol-rich Ld and Lo phases are less pronounced for these probes. Moreover, unlike 3-hydroxyflavone-based probes, Nile Red and NR12S are insensitive to the surface charge (DOPS vs DOPC) (Table 2). Thus, in contrast to the other mentioned probes, Nile Red and NR12S show a characteristic blue-shifted emission only in cholesterol-rich Lo phase.

The fluorescence quantum yield of the probes also depends on the phase state of the lipid membranes, especially in the case of probe NR12S. Indeed, the highest quantum yields are observed with the Ld phase, and the lowest ones are associated with the $L\beta$ phase. Because of its highly dense packing, the $L\beta$ phase is likely characterized by a relatively low number of binding sites for the probe, leading to a less efficient probe binding (so that a significant fraction of the probe is in bulk solution), which decreases the apparent fluorescence quantum yield of the probe. In contrast, the loosely packed Ld phase presents a much larger number of binding sites, thus explaining a more efficient probe binding accompanied by a higher fluorescence intensity. The Lo phase presents an intermediate case. The weaker dependence of the fluorescence quantum yield of Nile Red on the phase state is probably due to its smaller size and less specific binding to lipid bilayers as compared to NR12S, which ensures a sufficient number of binding sites independently of the membrane phase. Noticeably, in contrast to data in organic solvents, the emission of NR12S in all studied lipid vesicles is systematically blue-shifted with respect to Nile Red (Tables 1 and 2). This indicates that the fluorophore of NR12S is more deeply embedded in the bilayer than Nile Red, in line with our conclusions on a more specific binding of NR12S to lipid membranes.

To further characterize the sensitivity of the dyes to the Lo phase, the effect of temperature was investigated. In SM/CL vesicles at 60 °C, both NR12S and Nile Red show significantly red-shifted spectra compared to those at 20 °C (Table 2), confirming the strong sensitivity of the probes to the Lo → Ld transition. This transition also increases the fluorescence quantum yield of the NR12S probe, likely due to the increase in the number of the probe binding sites.

Thus, the experiments in model membranes show that the new probe similarly to the parent Nile Red is highly sensitive to the phase state of lipid bilayers and distinguishes Lo from Ld phases by the color of its emission.

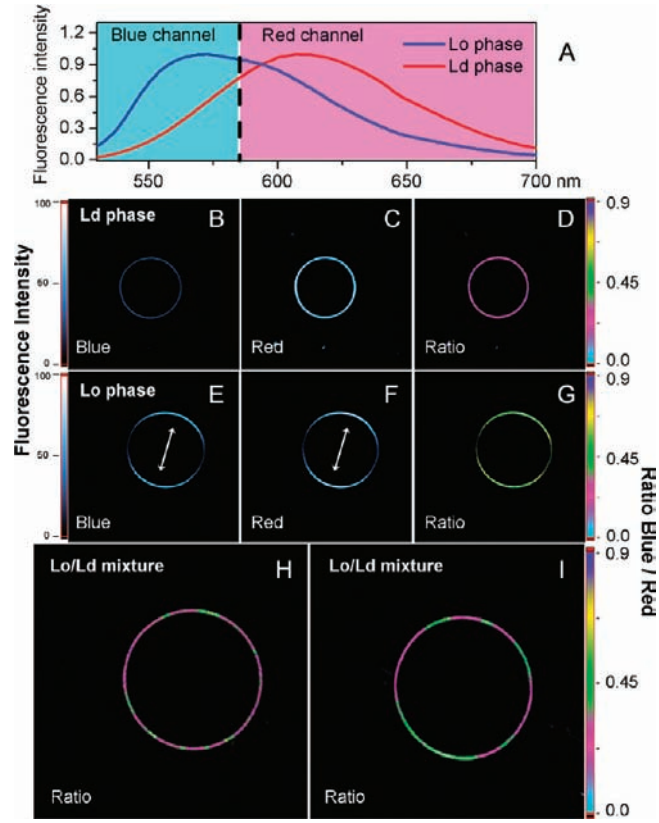


***Figure 6.*** Fluorescence microscopy imaging of Lo and Ld phases in GUVs using NR12S. (A) Normalized fluorescence spectra of NR12S in Ld (DOPC) and Lo (SM/Chol) phases of LUVs. The cyan and magenta regions separated at 585 nm represent the detection range for the blue and red channels of the microscope. GUVs were composed of DOPC (Ld phase: B, C, D), SM/Chol, 2/1 (Lo phase: E, F, G), and DOPC/SM/Chol, 1/1/0.7 (mixed Lo/Ld phases: H,I). Intensity images at the blue (<585 nm, B and E) and the red (>585 nm, C and F) channels. In the ratiometric images (D, G, H, and I), the color of each pixel represents the value of the intensity ratio $I_{blue}/I_{red}$, while the pixel intensity corresponds to the total intensity at both channels. Two-photon excitation wavelength was at 830 nm. Arrows indicate the orientation of the light polarization. Sizes of the images were 70 $\mu$m × 70 $\mu$m. Probe concentration was 1 $\mu$M.

**Imaging Cholesterol-Rich Phases in Giant Vesicles.** Because of their relatively large size (5−100 $\mu$m), giant vesicles (GUVs) are an excellent biomembrane model for fluorescence microscopy studies.[27] We thus performed two-photon fluorescence imaging of GUVs using NR12S, in order to evaluate its capability to visualize Ld and Lo phases. We first measured the two-photon absorption cross-section of Nile Red and NR12S at 830 nm using Rhodamine B as a standard as described previously (see Supporting Information).[37] The observed values 32 and 30 GM ($10^{-50}$ cm$^4$ × s × photon$^{-1}$) for Nile Red and NR12S, respectively, are sufficiently large for their application in two-photon microscopy.[37] Since the position of the emission maximum of NR12S changes in response to the phase state, ratiometric imaging[18,20] can be performed by splitting its emission into blue and red regions (Figure 6A). For the Ld phase (DOPC), the area under the NR12S emission spectrum in the blue region (<585 nm) is much smaller as compared to the red

(36) Massey, J. B. *Biochim. Biophys. Acta* **1998**, *1415*, 193–204.

(37) (a) Xu, C.; Webb, W. W. *J. Opt. Soc. Am. B* **1996**, *13*, 481–491. (b) Albota, M. A.; Xu, C.; Webb, W. W. *Appl. Opt.* **1998**, *37*, 7352–7356.

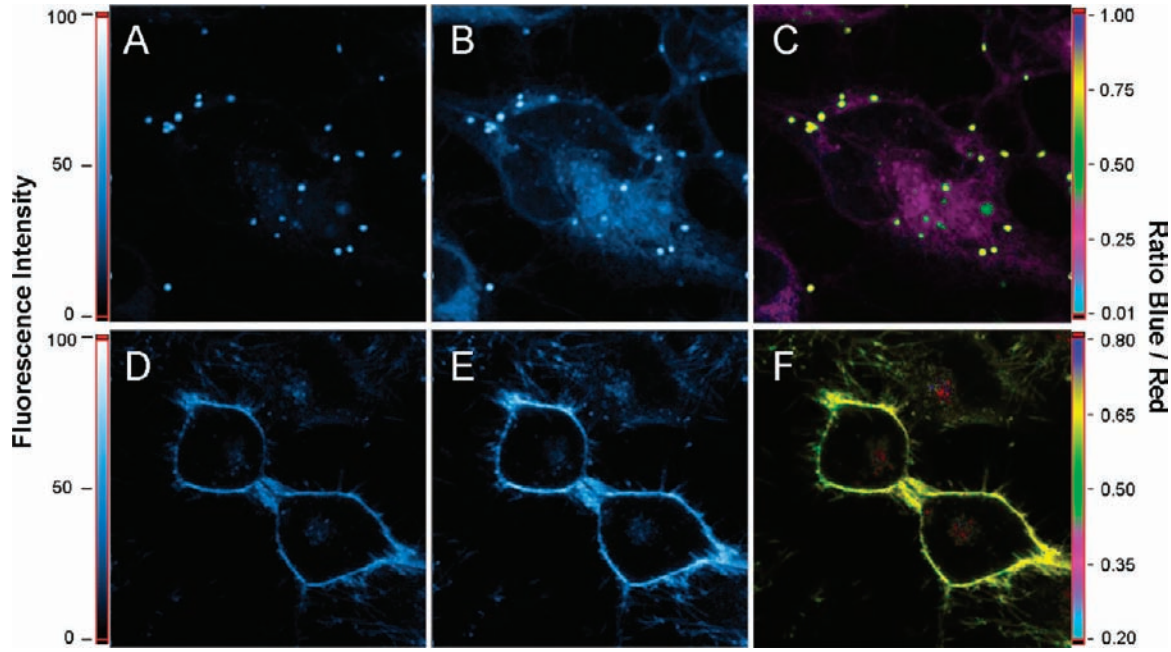


***Figure 7.*** Fluorescence intensity (A, B, D, E) and ratiometric (C, F) images of cells stained with Nile Red (A−C) and NR12S (D−F). Intensity images at the short-wavelength "blue" (<585 nm, A and D) and the long-wavelength "red" (>585 nm, B and E) channels are presented. In the ratiometric images, the color of the pixel represents the value of the intensity ratio of the blue channel to that of the red channel, while the pixel intensity corresponds to the total number of photons collected at both channels. Two-photon excitation wavelength was at 830 nm. Sizes of the images were 70 $\mu$m × 70 $\mu$m. Probe concentration was 0.3 $\mu$M.

region (>585 nm), so that the estimated ratio of the integral intensities $I_{blue}/I_{red}$ is ca. 0.23. In contrast, for Lo phase (SM/Chol), these areas are similar, and the corresponding $I_{blue}/I_{red}$ value is ca. 0.88. This 4-fold difference in the ratio should be easily detectable by a fluorescence microscope having blue (<585 nm) and red (>585 nm) detection channels. In line with these expectations, the fluorescence images of the equatorial section of GUVs composed of DOPC (Ld phase) show that the intensity at the blue channel is much lower than at the red channel (Figure 6B and C), while for SM/Chol GUVs (Lo phase) these intensities are comparable (Figure 6E and F). In the ratiometric images, the GUV membranes in Ld phase appear predominantly in pink pseudocolor corresponding to a ratio around 0.20−0.25 (Figure 6D), which matches perfectly the predicted ratio from the fluorescence spectra. For Lo phase, GUV membranes appear in green-yellow pseudocolor corresponding to a ratio around 0.62−0.67 (Figure 6G), which also matches well the expected ratio.

Importantly, the ratiometric images of GUVs composed of DOPC/SM/Chol (1/1/0.7 molar ratios) present clear separated domains with two different pseudocolors (Figure 6H and I). These pseudocolors correspond well to those observed in pure Ld and Lo phases, which allows unambiguous assignment of the pink domains (low $I_{blue}/I_{red}$ ratio) to Ld phase and the green domains (high $I_{blue}/I_{red}$ ratio) to Lo phase. Importantly, the high fluorescence intensity from both Lo and Ld phases in the ternary mixture suggests that NR12S partitions evenly between them, though it is difficult to estimate the exact partition ratio. Since most fluorescent dyes preferentially bind Ld phase in ternary mixtures,[17] the even distribution of NR12S between Lo and Ld phases is an important advantage for their simultaneous visualization. Only few environment-sensitive dyes show this ability: Prodan derivatives, styrylpyrydinium dyes and, to lesser extent, 3-hydroxyflavone derivatives.[18–21]

Noticeably, while the fluorescence intensity of NR12S is homogeneously distributed all over the DOPC GUV membrane (Figure 6B and C), it depends on the orientation of the bilayer plane with respect to the polarization plane of the excitation light in SM/Chol GUVs (Figure 6E and F). In line with already reported data for other environment-sensitive and rod-shaped probes,[18,19,21a] the fluorescence intensity of NR12S in Lo phase is the highest when the light polarization is parallel to the probe fluorophore exhibiting preferentially vertical orientation due to the constrained lipid packing. In contrast, the loosely packed Ld phase of DOPC membrane imposes no preferential orientation for the fluorophore, so that efficient probe excitation can always be achieved.

**Cellular Studies.** Two-photon fluorescence imaging of living cells stained with the probes shows that Nile Red exhibits mainly intracellular fluorescence (Figure 7A−C), which according to the literature corresponds to a staining of lipid droplets.[23] Remarkably, the fluorescence ratio (blue/red channels) from the intracellular droplets is much larger than from other parts of the cell, in line with their highly apolar nature. In contrast, the new probe NR12S stains exclusively the cell plasma membrane, as it can be seen from the typical membrane staining profile and the rather uniform fluorescence intensity ratio within the image (Figure 7D−F). Thus, the conjugation of the Nile Red fluorophore with the detergent-like anchor group allows localizing the fluorophore on the cell membrane. Moreover, addition of 10 mM dithionite results in >90% bleaching of NR12S bound to the cells (see Supporting Information), showing a specific binding to the outer leaflet of the plasma membrane with almost no internalization into the cell.

The new probe showing high binding specificity together with high sensitivity to the membrane phase appears thus as an attractive tool for studying the lipid phases at the outer leaflet of living cells. The fluorescence maximum of NR12S in intact

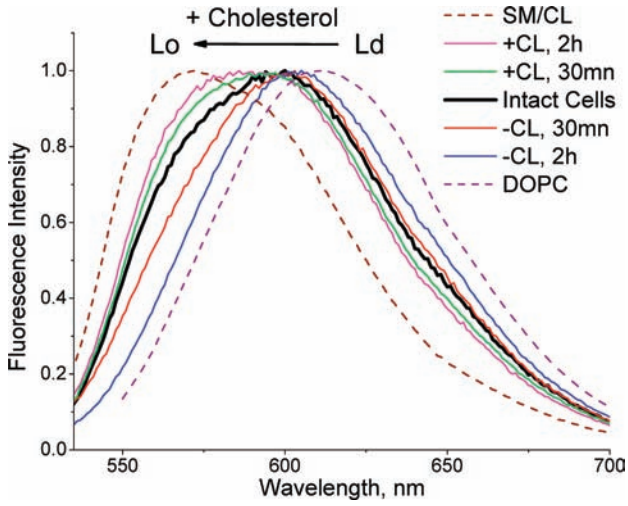


***Figure 8.*** Normalized fluorescence spectra of 0.1 $\mu$M NR12S in cells at different levels of cholesterol depletion/enrichment and in model membranes presenting Lo (SM/CL) and Ld (DOPC) phases.

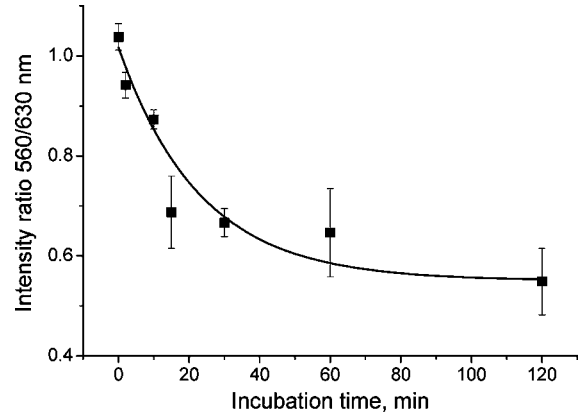


***Figure 9.*** Monitoring the kinetics of cholesterol extraction from astrocytoma cells using NR12S probe. Ratio of the emission intensities at 560 and 630 nm of NR12S in cells treated with 5 mM M$\beta$CD for different times. The curve represents a single exponential fit to the experimental data. Each data point is the average of three measurements.

cells is intermediate to those with the Lo and Ld phases of model membranes (Figure 8), in line with the high content in plasma membranes of unsaturated lipids, sphingomyelin and cholesterol favoring both phases.[1,10] Other reports also suggested a significant fraction of Lo phase in the cell plasma membranes.[38] Importantly, the emission maximum of NR12S is stable for 30 min, confirming that flip-flop and internalization of the probe are relatively slow. Since cholesterol is a key component of the Lo phase, we modified its content in cell membranes, using methyl-$\beta$-cyclodextrin (M$\beta$CD).[11,28] On cholesterol depletion, the NR12S probe shows a red shift (Figure 8), so that the obtained spectrum is close to that with the Ld phase vesicles (DOPC, Figure 8). As NR12S is rather insensitive to cholesterol variation within Ld phase (see above), it likely reports on the disappearance of the Lo phase after cholesterol depletion. It should be noted that the present data do not provide a proof for the presence of separated Lo phase domains in cell membranes. Indeed, cell membranes can present a special phase, having features of both Lo and Ld phases, which can be converted into Ld phase after cholesterol depletion. Importantly, the red shift value depends on the incubation time of the cells with M$\beta$CD, suggesting an application of NR12S for a quantitative description of cholesterol depletion.

In order to monitor the kinetics of cholesterol depletion, we took the intensity ratio at the blue and red sides of the NR12S spectra, namely, 560 and 630 nm, where the variations of the relative intensities are maximal (Figure 8). Incubation with 5 mM M$\beta$CD results in a relatively rapid decrease in the intensity ratio 560/630 nm within the first 15 min, followed by slower changes at longer incubation times (Figure 9). Fitting the data to a single exponential decay provided a cholesterol depletion time constant of 23 $\pm$ 6 min, in excellent agreement with the half-time of 21 $\pm$ 6 min obtained previously from extraction of $^3$H-labeled cholesterol with 2-hydroxypropyl-$\beta$-cyclodextrin.[11a] Other reports on model[39] and cellular membranes[11b,28] also suggest a similar time scale of cholesterol depletion, though the rate of the process depends strongly on the initial cholesterol content. The correspondence of our data with the literature shows that our method using NR12S can quantify cholesterol in cell membranes and describe its depletion kinetics.

In contrast to its depletion, cholesterol enrichment in living cells using M$\beta$CD−cholesterol complex shifts the NR12S emission to the blue, so that the obtained spectrum becomes closer to that of model vesicles presenting a homogeneous Lo phase (SM/CL, Figure 8). The spectroscopic effect increases with the time of incubation with the M$\beta$CD−cholesterol complex. Thus, the new probe can monitor in a rather broad range the cholesterol content and the fraction of cholesterol-rich Lo phase in cell membranes.

To visualize cells at different concentrations of cholesterol, we performed fluorescence ratiometric imaging before and after treatment with M$\beta$CD. After cholesterol depletion, there is a clear change in the pseudocolor of the cells, indicating a decrease in the intensity ratio recorded at the blue (<585 nm) and the red (>585 nm) parts of the probe emission spectrum (Figure 10). This decrease is in agreement with the red shift of the fluorescence spectra in cell suspensions (Figure 8). It can be also noticed that after cholesterol depletion, the cells differ one from another by their blue/red intensity ratio (Figure 10C), suggesting that the efficiency of cholesterol extraction varies from cell to cell. Moreover, after cholesterol extraction the cell membranes appear smoother, so that the numerous extensions of cell membranes are no more observed (Figure 10). These changes in morphology can be attributed to the disruption of the native cytoskeleton, which is highly cholesterol-dependent.[40] It can also be noted that neither intact cells nor cells treated with M$\beta$CD show membrane heterogeneity, which one would expect from separated Lo/Ld phase domains in the microscopic scale. Thus, though our data suggests the presence of

(38) (a) Hao, M.; Mukherjee, S.; Maxfield, F. R. *Proc. Natl. Acad. Sci. U.S.A.* **2001**, *98*, 13072–13077. (b) Gidwani, A.; Holowka, D.; Baird, D. *Biochemistry* **2001**, *40*, 12422–12429. (c) Swamy, M. J.; Ciani, L.; Ge, M.; Smith, A. K.; Holowka, D.; Baird, B.; Freed, J. H. *Biophys. J.* **2006**, *90*, 4452–4465. (d) Oncul, S.; Klymchenko, A. S.; Kucherak, O. A.; DemchenkoA. P.; Martin, S.; Dontenwill, M.; Arntz, Y.; Didier, P.; Duportail, G.; Mély, Y. *Biochim. Biophys. Acta* **2010**, in press, doi: 10.1016/j.bbamem.2010.01.013.

(39) Radhakrishnan, A.; McConnell, H. M. *Biochemistry* **2000**, *39*, 8119–8124.

(40) (a) Martin, S.; Phillips, D. C.; Szekely-Szucs, K.; Elghazi, L.; Desmots, F.; Houghton, J. A. *Cancer Res.* **2005**, *65*, 11447–11458. (b) Ramprasad, O. G.; Srinivas, G.; Rao, K. S.; Joshi, P.; Thiery, J. P.; Dufour, S.; Pande, G. *Cell Motil. Cytoskeleton* **2007**, *64*, 199–216. (c) Patra, S. K. *Biochim. Biophys. Acta* **2008**, *1785*, 182–206.

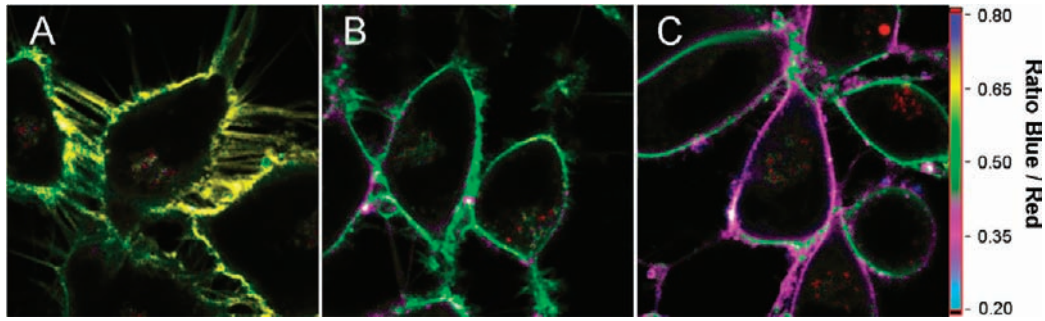


***Figure 10.*** Fluorescence ratiometric images of cells stained with NR12S at different levels of cholesterol depletion. Intact cells (A) and cells after incubation with 5 mM M$\beta$CD for 30 min (B) and 2 h (C). The color of each pixel represents the value of the intensity ratio of the blue to the red channel, while the pixel intensity corresponds to the total number of photons collected at both channels. Two-photon excitation wavelength was at 830 nm. Sizes of the images were 50 $\times$ 50 $\mu$m. Probe concentration was 0.3 $\mu$M.

cholesterol-rich Lo phase in cell membranes, we cannot visualize separated domains with optical microscopy. The hypothetic Lo phase domains, if they exist, are probably too small and dynamic to be detected in our fluorescence images, due to the limited spatial and temporal resolution of the imaging technique.[41]

## Conclusions

A probe based on Nile Red has been synthesized for studying cholesterol and lipid order in biomembranes. Unlike the parent Nile Red, the new probe binds spontaneously to the outer leaflet of model and cell plasma membranes with very slow flip-flop and internalization. Spectroscopy studies of LUVs and fluorescence imaging of GUVs further show that the probe can distinguish by its emission color between liquid ordered and disordered phases. Using cholesterol depletion/enrichment with methyl-$\beta$-cyclodextrin, we showed that the emission color of this probe correlates well with the cholesterol content in cell membranes. The key advantages of the new probe compared to existing membranes probes arise from its Nile Red fluorophore: superior brightness, red-shifted absorption and emission, high photostability and on/off switching capability. These properties make the new probe a powerful tool for monitoring cholesterol and lipid order selectively at the outer leaflet of cell membranes.

**Acknowledgment.** This work was supported by Conectus Alsace and ANR blanc grants.

**Supporting Information Available:** Synthesis of NR12S, additional data on bleaching by dithionite, and two-photon absorption cross section results. This material is available free of charge via the Internet at http://pubs.acs.org.

JA100351W

(41) (a) Lenne, P. F.; Wawrezinieck, L.; Conchonaud, F.; Wurtz, O.; Boned, A.; Guo, X. J.; Rigneault, H.; He, H. T.; Marguet, D. *EMBO J.* **2006**, *25*, 3245–3256. (b) Wawrezinieck, L.; Rigneault, H.; Marguet, D.; Lenne, P. F. *Biophys. J.* **2005**, *89*, 4029–4042. (c) Veatch, S. L.; Cicuta, P.; Sengupta, P.; Honerkamp-Smith, A.; Holowka, D.; Baird, B. *ACS Chem. Biol.* **2008**, *3*, 287–293.